



Universiteit
Leiden
The Netherlands

High velocity instabilities in the vortex lattice of Nb/permalloy bilayers

Armenio, A.A.; Bell, C.; Aarts, J.; Attanasio, C.

Citation

Armenio, A. A., Bell, C., Aarts, J., & Attanasio, C. (2007). High velocity instabilities in the vortex lattice of Nb/permalloy bilayers. *Physical Review B*, 76, 054502.
doi:10.1103/PhysRevB.76.054502

Version: Not Applicable (or Unknown)

License: [Leiden University Non-exclusive license](#)

Downloaded from: <https://hdl.handle.net/1887/45421>

Note: To cite this publication please use the final published version (if applicable).

High-velocity instabilities in the vortex lattice of Nb/permalloy bilayers

A. Angrisani Armenio,¹ C. Bell,² J. Aarts,² and C. Attanasio¹

¹Laboratorio Regionale SuperMat, CNR-INFM Salerno, and Dipartimento di Fisica "E. R. Caianiello," Università degli Studi di Salerno, Baronissi, Salerno I-84081, Italy

²Kamerlingh Onnes Laboratory, Leiden University, P.O. Box 9504, 2300 RA Leiden, The Netherlands

(Received 13 April 2007; revised manuscript received 11 June 2007; published 1 August 2007)

We have studied the critical current density J_c for onset of vortex motion and the dynamic instability of the moving vortex lattice at high driving currents in superconducting (S)/ferromagnetic (F) Nb/Ni_{0.80}Fe_{0.20} bilayers and in a single Nb film with the same thickness. The samples are all characterized by relatively high values of the pinning strength. The measured current-voltage characteristics are successfully described in the framework of the Larkin-Ovchinnikov model, modified in order to take into account the effect of the pinning close to the instability. We find that J_c is smaller in the S/F bilayers than in the single film and argue that this is due to the strongly inhomogeneous order parameter in the bilayers. Also, the critical velocity v^* for the occurrence of the instability is found to be significantly larger in the S/F bilayers than in the single S layer. By extracting the quasiparticle energy relaxation rate from v^* , we show that this effect is due to the same inhomogeneous order parameter and the resulting lower average value of the superconducting gap.

DOI: 10.1103/PhysRevB.76.054502

PACS number(s): 74.45.+c, 74.78.-w, 74.78.Fk

I. INTRODUCTION

The interplay between a superconductor (S) and a ferromagnet (F) through the proximity effect in artificial S/F hybrids is currently a very active field of research involving both fundamental and application aspects.¹ One of the peculiarities of S/F hybrids is the strongly inhomogeneous nature of the superconducting order parameter. On the F side of the interface, the interaction of the exchange field with the Cooper pairs causes the order parameter to oscillate,^{1,2} whereas on the S side, the order parameter is strongly suppressed over a distance of the order of the superconducting coherence length ξ_S , which is usually a few nanometers. The best known consequences of this highly inhomogeneous character of the order parameter are the strong suppression of the superconducting critical temperature T_c with decreasing S-layer thickness d_S , and the nonmonotonic behavior of T_c as function of the thickness d_F of the F layer,³ while in S/F/S Josephson junctions, negative critical currents appear.^{4,5} The nonhomogeneous character of the order parameter was also recently studied by measuring the depairing current density J_{dp} , which is determined by an average of the superconducting order parameter over the layer thickness.^{6,7}

Such averaging should manifest itself also in other properties of the bilayer system. For instance, the force to pin vortices in the superconductor can be expected to be different, which is observable by measuring the onset of voltage at the so-called critical current in the current (I)-voltage (V) characteristic. Differences should also be found in behavior of the moving vortex system. In particular, at high vortex velocities, an instability can occur, which drives the system to the normal state and therefore manifests itself by a jump in the voltage. This instability, first described by Larkin and Ovchinnikov (LO),⁸ is related to the inelastic relaxation rate τ_E of quasiparticles inside the vortex core. Such instabilities have been observed in a number of systems including low-temperature⁹⁻¹² and high-temperature superconducting thin films¹³⁻¹⁶ and multilayers.¹⁷⁻¹⁹ What essentially emerges

from these studies is that the voltage jumps are indeed due to intrinsic properties of the moving vortex lattice but that two more ingredients may play a role, (i) the temperature dependence of τ_E , in particular, when electron-electron interactions dominate the relaxation, and (ii) vortex pinning, ignored in the original LO theory.²⁰ The LO theory has been also extended to explicitly consider the contributions due to the heating effect.²¹ Finally, measurements of flux-flow instabilities have been recently used to extract information about the symmetry of the order parameter in YBa₂Cu₃O₇ thin films.^{22,23}

In the present paper, we study LO instabilities in S/F bilayers of Nb/Ni_{0.80}Fe_{0.20}, and for comparison in a single Nb film, by measuring their I - V characteristics in perpendicular magnetic fields. Using Ni_{0.80}Fe_{0.20} (Permalloy), a strong ferromagnet, ensures that the order parameter is strongly suppressed at the interface, so that the effects of the inhomogeneous order parameter can be investigated. The outline of the paper is as follows. First, we give the theoretical framework to describe and analyze the flux-flow instabilities, followed by some experimental details. Results are then presented on the critical current density J_c for the onset of vortex motion and on the critical velocity v^* where the instability occurs. From the analysis of the instabilities as a function of the temperature and magnetic field, we establish the role played by the ferromagnet in determining the nonequilibrium Nb properties.

II. VORTEX LATTICE INSTABILITIES

In the case of a vortex lattice moving under high applied driving currents, Larkin and Ovchinnikov theoretically predicted a sudden voltage jump in the I - V curves before reaching the value of the depairing current I_{dp} .⁸ This fact is important not only from a fundamental point of view but it has also practical implications because it establishes a limit for the sustainable current in the superconducting state. The abrupt switching of the sample to a state of higher electrical

resistance is caused by the electric field generated by the vortex motion, which shifts the distribution of quasiparticles inside the core to higher energies, causing some of them to leave the core all together. The vortex core therefore shrinks with increasing flux-line velocity v , and the viscous damping coefficient decreases. For a critical value of the velocity v^* , the flux-flow state becomes unstable and the system switches to the normal state. The amount of decrease of the damping is controlled by the energy relaxation time of the quasiparticles τ_E . For the viscous damping coefficient η as function of the vortex velocity v , LO obtained the expression

$$\eta(v) = \eta(0) \frac{1}{1 + (v/v^*)^2}, \quad (1)$$

where $\eta(0)$ is the viscous damping coefficient at zero velocity. From Eq. (1), one sees that the damping force $F_v = v\eta$ increases with increasing velocity until it reaches a maximum at $v = v^*$. Since v is proportional to the voltage V through the Lorentz force, the current-voltage characteristics are, according to LO, described by the relation

$$\frac{V}{1 + (V/V^*)^2} + cV(1-t)^{1/2} = (I - I_c)R_{ff}, \quad (2)$$

where $t = T/T_c$ is the reduced temperature, I_c is the critical current, R_{ff} is the flux-flow resistance, and c is a constant of the order of unity. The curve starts to bend upward in the vicinity of the critical voltage V^* , which is related to v^* by means of the relation

$$V^* = \mu_0 v^* H L, \quad (3)$$

where H is the applied magnetic field and L is the distance between the voltage contacts.

For the critical velocity LO found

$$v^* = \frac{D^{1/2} [14\zeta(3)]^{1/4} (1-t)^{1/4}}{(\pi\tau_E)^{1/2}}, \quad (4)$$

where $\zeta(x)$ is the Riemann zeta function and D is the *quasi-particle* diffusion coefficient, which means that from measuring the critical voltage V^* it is possible to estimate values for τ_E . As can be expected, faster relaxation (smaller τ_E) leads to larger v^* . In this respect, it is important to note that a temperature dependence can also be expected for τ_E . If the dominant relaxation mechanism is electron-phonon scattering, it should be $\tau_E \propto T^{-3}$, while if electron-electron interactions dominate, it is $\tau_E = \tau_{E,el} \exp[2\Delta(T)/k_B T]$, where $\tau_{E,el}$ is basically the inelastic relaxation time of the electron system, and $\Delta(T)$ has the temperature dependence $\Delta(T) = \Delta(0)(1 - T/T_c)^{1/2}$ from the BCS theory. This exponential behavior for τ_E was indeed found in various materials, with $\Delta(0) = 1.76k_B T_c$ as expected from the BCS theory for low- T_c amorphous Mo_3Si and $\Delta(0) = 3.5k_B T_c$ for high- T_c $\text{YBa}_2\text{Cu}_3\text{O}_7$ (Ref. 14) in accordance with the enhanced gap values in high- T_c materials. In Ta/Ge multilayers, again $\Delta(0) = 1.76k_B T_c$ was found when the Ta layers were uncoupled, while a coupled anisotropic multilayer yielded $\Delta(0) = 3.5k_B T_c$,¹⁸ indicating that the anisotropy leads to an

effective value for $\Delta(0)$ without changing the exponential dependence.

Another point to note is that in the LO theory, the critical velocity [Eq. (4)] should not be dependent on the external magnetic field.⁸ However, it was discussed that the LO condition for a spatially homogeneous quasiparticle nonequilibrium distribution is only met when the distance $v^* \tau_E$ is larger than the intervortex distance a_0 . At low magnetic fields, this is not the case, and v^* becomes proportional to a_0 and therefore to $\sqrt{1/H}$.¹⁴ The crossover between the two regimes takes place when

$$v^* \tau_E = a_0 f(T), \quad (5)$$

where $f(T)$ is a numerical factor of the order of unity.

III. EXPERIMENT

A Nb film and Nb/Py bilayers were prepared by dc sputter deposition on oxidized Si(100) substrates in an ultrahigh vacuum system.²⁴ We studied one single 25 nm thick Nb film and two bilayers with the same Nb thickness $d_{\text{Nb}} = 25$ nm and Py thickness $d_{\text{Py}} = 10$ and 75 nm, respectively. As we will see, in all samples, the pinning is relatively high, with the low-field critical current density values higher than 10^9 A/m² at $t = T/T_c = 0.5$. Py, apart from having a quite large spin polarization²⁵ is characterized by very small values of the coercive fields H_c at low temperatures, slightly dependent on thickness. Typical values for H_c in our samples, measured with an in-plane field, are around 2 mT (10 mT) for 50 nm (20 nm) thick Py films.²⁶ The low coercivity, the preferential in-plane magnetization, and the very small thickness make that domain configurations or flux variations in the superconductor due to the ferromagnet do not play a role in our experiments, which are carried out in perpendicular applied field. Even a small in-plane field, for instance, due to external stray fields or a small misalignment of the sample normal with respect to the applied field, will drive out the domains and make the in-plane magnetization uniform. The large demagnetization factor then ascertains that the amount of flux produced by the small volume of the ferromagnetic layer is negligible; in other words, the magnetic induction equals the applied field.

To measure the I - V curves, using the standard dc four-probe technique, the samples were structured by e-beam lithography into strips with width $w = 10$ μm . The length between the voltage contacts was 100 μm . The I - V curves were measured by putting the samples in direct contact with the liquid helium to minimize any heating effect. The measurements were performed by sending current rectangular pulses to the samples. The current-on time was of 12 ms followed by a current-off time of 1 s. Any single voltage value was acquired at the maximum value of the current. The above procedure was repeated by sweeping the currents upward and then downward, and no hysteresis in the curves was detected. This indicates that the instability detected in the I - V characteristics has no thermal origin. The magnetic field was applied perpendicular both to the plane of the substrate and to the direction of the current. As a first characterization, the superconducting transition temperature T_c and

TABLE I. Characteristic parameters of the measured samples. d_{Nb} (d_{Py}) is the Nb (Py) layer thickness, T_c is the critical temperature, ρ_n is the normal state resistivity measured at $T=10$ K, $H_{c2\perp}(t=0.5)$ is the value of the perpendicular critical field at the reduced temperature equal to 0.5, and D is the quasiparticle diffusion coefficient as determined from the $H_{c2\perp}$ versus temperature curve for the single Nb film.

Sample	d_{Nb} (nm)	d_{Py} (nm)	T_c (K)
Nb	25	0	8.59
NbPy10	25	10	6.97
NbPy75	25	75	6.72

	ρ_n ($\mu\Omega$ cm)	$H_{c2\perp}$ ($t=0.5$)(T)	D (m^2/s)
Nb	7.4	1.75	2.78×10^{-4}
NbPy10	2.4	0.75	
NbPy75	6.7	0.75	

the temperature dependence of the perpendicular upper critical magnetic fields $H_{c2\perp}(T)$ were resistively measured in the four contact configuration; the values were extracted from the $R(T)$ curves, taking the 90% value of the normal state resistance R_N just above the transition to the superconducting state. The transition widths, estimated from the temperature difference at 10% and 90% of R_N , were typically less than 60 mK at zero field and did not substantially broaden, even in high perpendicular magnetic fields, confirming the high quality of our samples. From the slope of the perpendicular upper critical field,²⁷ it is also possible to estimate the quasiparticle diffusion coefficient $D=(4k_B/\pi e) \times (-dH_{c2\perp}/dT|_{T=T_c})^{-1}$ for the single Nb film. Because in layered S/F systems the $H_{c2\perp}(T)$ curves shift in a parallel way as a function of the layer thicknesses, the slope of the perpendicular upper critical field cannot be used directly to determine D for the two Nb/Py bilayers.^{28,29} We will take D for Nb for all the calculations. Some characteristic parameters of the measured samples are reported in Table I. Note that T_c for the bilayers has decreased by about 1.5 K, which means that the order parameter, assumed to be close to zero at the interface, has relaxed substantially to the bulk value. We therefore expect it to be inhomogeneous over the full film thickness.

IV. RESULTS AND DISCUSSION

A. Critical currents

In Fig. 1(a), the I - V characteristics are shown for the single Nb film at $t=0.5$ for different values of the external magnetic field between 0.05 and 1.8 T as indicated. Up to a certain value of the magnetic field, the curves exhibit a sudden jump at a well defined current value I^* , well above the critical current I_c where the onset of voltage occurs. At higher magnetic fields, the I - V curves become more smeared and finally the jump disappears. This observation is consistent with other results found on different kinds of supercon-

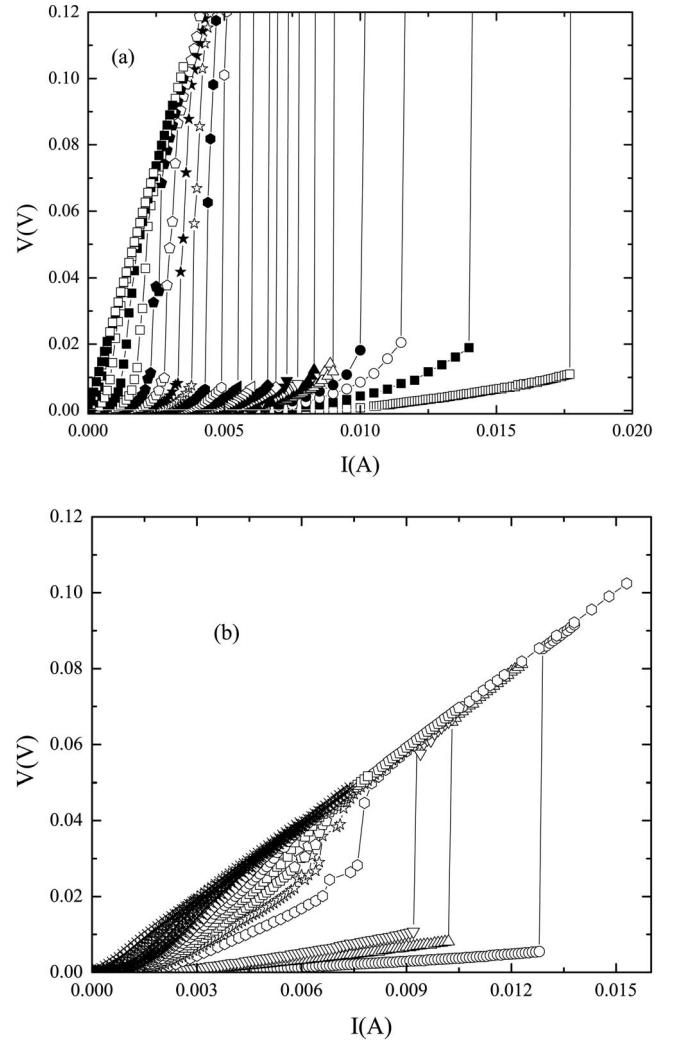


FIG. 1. (a) I - V curves for the Nb film at $t=T/T_c=0.5$ for different values of the external field. The magnetic fields are, from right to left, 0.05, 0.1, 0.15, 0.2, 0.25, 0.3, 0.35, 0.4, 0.45, 0.5, 0.6, 0.7, 0.8, 0.9, 1.0, 1.1, 1.2, 1.3, 1.4, 1.5, 1.6, 1.7, 1.75, and 1.8 T. (b) I - V curves for the NbPy75 bilayer at $t=T/T_c=0.5$ for different values of the external field. The magnetic fields are, from right to left, 0.01, 0.02, 0.03, 0.04, 0.05, 0.075, 0.1, 0.15, 0.2, 0.25, 0.3, 0.35, 0.4, 0.45, 0.5, 0.6, 0.7, and 0.75 T.

ducting systems.⁹⁻¹⁹ Very similar behavior is observed for both Nb/Py bilayers. In Fig. 1(b), we show the I - V curves, also measured at $t=0.5$, for the NbPy75 sample.

The critical current density $J_c=I_c/(wd)$ (d is the sample thickness) at $t=0.5$ for the three samples is shown in Fig. 2 as a function of the external magnetic field. The critical current I_c was defined using a dc voltage criterion of $2 \mu\text{V}$. For all samples, J_c rises quickly when the field is lowered below H_{c2} and becomes more or less constant below $H_{c2}/2$. At these low fields, where the pinning is individual rather than collective, the values for J_c range from $10^9 \text{A}/\text{m}^2$ for NbPy75 to $5 \times 10^{10} \text{A}/\text{m}^2$ for Nb. The pinning is therefore quite strong in comparison, for instance, with amorphous materials. Also, the values for the two Nb/Py bilayers are substantially smaller than for the single film and we want to argue that this is an immediate consequence of the *homogeneous*

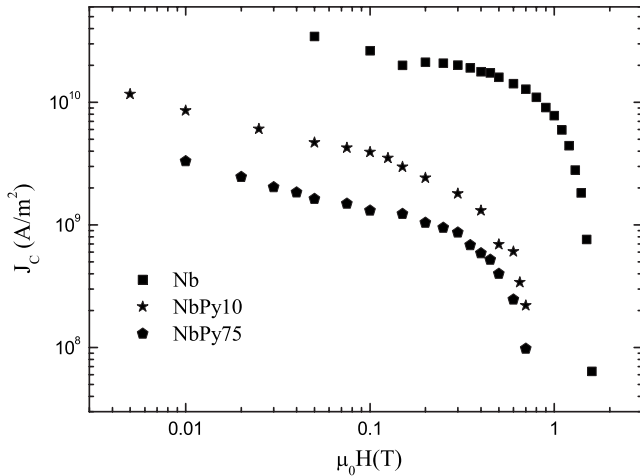


FIG. 2. Critical current density versus perpendicular magnetic field at $t=0.5$ for the three analyzed samples.

suppression of the order parameter inside the Nb. The single-vortex pinning in superconducting films is due to defects in the crystal lattice which can be pointlike or extended (grain boundaries) and which cause local variations in the order parameter. Such defects pin vortices because of the smaller amount of condensation energy which locally has to be paid when the vortex resides there. In the region of homogeneously suppressed superconductivity, which is basically the whole film, the local energy gain is less, and the pinning consequently weaker. We want to note that this is opposite to what can be expected for a magnetic impurity in the superconducting matrix. In that case, the local suppression is stronger than that of ordinary defects and the pinning will be stronger, as was indeed found in NbTi wires with Ni and Fe impurities.³⁰ The effect is also opposite to the effect from domain walls in the ferromagnet which can pin a vortex by its flux.^{31,32}

Although not central to the paper, we can also remark that the relatively strong pinning in all samples appears to determine the precise shape of the I - V curves. Equation (2), for $I > I_c$, describes the I - V curves close to the instability only when pinning mechanisms are absent and in high enough fields that the flux-flow resistance ρ_f is given by the Bardeen-Stephen limit $\rho_f = \rho_n H / H_{c2}$, with ρ_n the normal state resistivity. To include the effect of low fields and pinning, the I - V relation should be modified as follows¹⁸:

$$I = \frac{V}{R_n} \left[\frac{\alpha(1 + \beta V^{-c})}{1 + (V/V^*)^2} + 1 \right], \quad (6)$$

where α , β , and c are constants and used as fitting parameters. The constant α corrects for the low-field flux-flow resistance; the other two constants parametrize the correction to the viscosity constant by the pinning. In Figs. 3(a) and 3(b), we show the initial part of the I - V curves close to the instability, for the Nb film and for the NbPy75 bilayer, respectively. The solid lines are the fits to the experimental points obtained by using Eq. (6). The fits are good, and the values obtained for the parameter α are quite small (around 10 or less) for all the magnetic fields in agreement with the

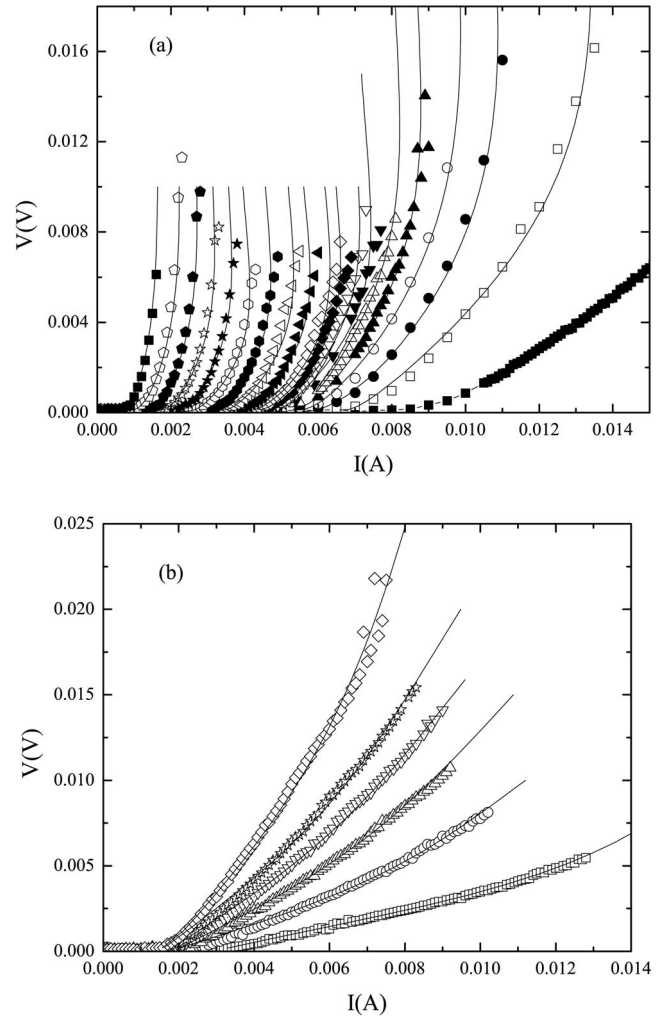


FIG. 3. (a) I - V curves for the Nb film close to the instability at $t=0.5$. The magnetic fields are, from right to left, 0.05, 0.1, 0.15, 0.2, 0.25, 0.3, 0.35, 0.4, 0.45, 0.5, 0.6, 0.7, 0.8, 0.9, 1.0, 1.1, 1.2, 1.3, and 1.4 T. The solid lines are fit to the experimental data obtained using Eq. (6). (b) I - V curves for the NbPy75 bilayer close to the instability at $t=0.5$. The magnetic fields are, from right to left, 0.01, 0.02, 0.03, 0.04, 0.05, and 0.075 T. The solid lines are fit to the experimental data obtained using Eq. (6).

results reported for high-pinning multilayers.¹⁸ Also, with the obtained values for α , β , and c , the theoretical curves do not show any back bending which results in hysteresis not due to thermal origin in the I - V characteristics.^{10,18} Such hysteresis has been observed on amorphous Mo₃Si for which, however, the estimated value for the parameter α was equal to 14.¹⁰

B. Critical velocities

Next, we come to the analysis of the critical velocities. We interpret the voltage V^* corresponding to the value of the current I^* , where the jumps in the I - V curves appear, as the LO flux-flow instability at the velocity v^* . The values of v^* , as obtained directly from the measured V^* using Eq. (3), are plotted as a function of H for the single Nb film and for the two Nb/Py bilayers in Figs. 4(a) and 4(b), respectively. In the insets, the behavior of v^* versus $H^{-1/2}$ at $t=0.5$ for the three

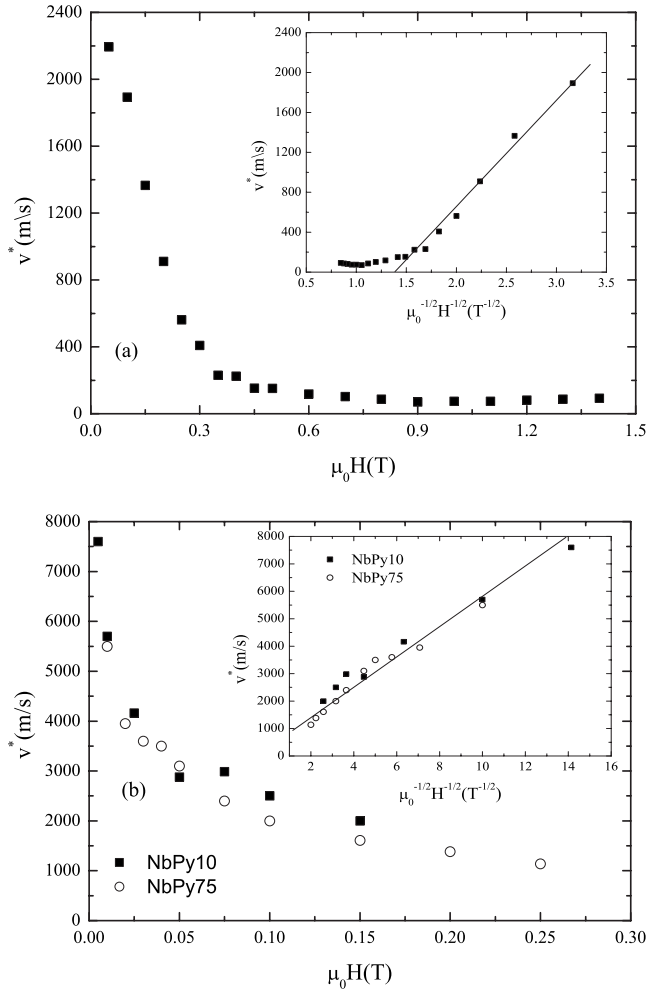


FIG. 4. Critical velocity v^* versus applied magnetic field at $t = 0.5$ (a) for Nb film and (b) for the two Nb/Py bilayers. Insets: v^* versus $H^{-1/2}$ at $t = 0.5$ (a) for Nb film and (b) for the two Nb/Py bilayers. The solid lines are guides to the eyes to show the $H^{-1/2}$ proportionality of v^* .

samples is shown. In both cases, the data in low fields show the critical velocity to be proportional to $H^{-1/2}$, indicating that thermal effects are not responsible for the observed instability. For the Nb film, also the crossover to a field-independent v^* is found. For the Nb/Py bilayers, the instability disappears already at field around 0.15 T, and we cannot detect the crossover. The numbers show that the critical velocities in the case of the Nb/Py bilayers are much larger and the instability disappears in this case already at smaller fields because the critical voltage V^* is always much closer to V_N (the normal state voltage) with respect to what happens in the single Nb film. Also, no substantial difference appears in the results obtained on the two Nb/Py bilayers. This is probably not surprising since Py is characterized by an induced superconducting coherence length of the order of only 1 nm.³³ However, as noticed in the literature,^{12,18,21} the $H^{-1/2}$ dependence of v^* can also be induced by unavoidable Joule heating. In this case, a well defined theoretical expression is predicted for the dissipated power $P^* = I^* V^*$ as a function of H/H_T .^{12,15,21} Here, I^* is the current value where instabilities take place and H_T is a characteristic magnetic field where

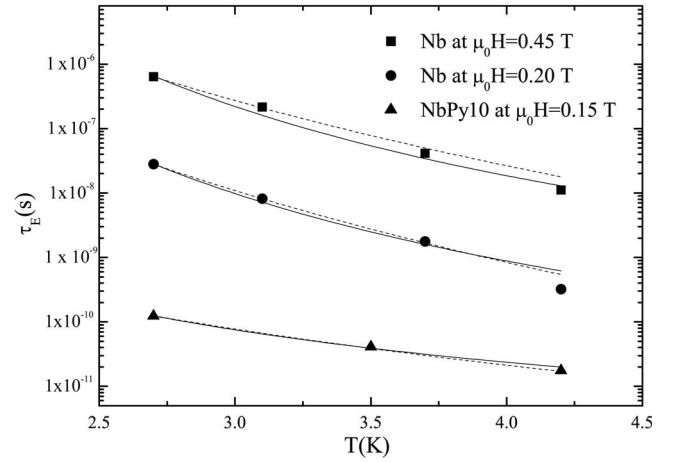


FIG. 5. τ_E temperature dependence for the Nb single film at $\mu_0 H = 0.45$ T and $\mu_0 H = 0.20$ T and for NbPy10 at $\mu_0 H = 0.15$ T. The dashed lines are the fit to the experimental data using the expression $\tau_E \propto T^{-n}$, while the solid lines are the fitting curves obtained using the formula $\tau_E = \tau_{E,el} \exp[m\Delta(T)/k_B T]$ (see the text for details).

thermal effects start to strongly influence the flux-flow instabilities. We did not find any agreement between theory and experiment for the Nb film, while in the case of both the Nb/Py samples, we get $\mu_0 H_T = 0.20$ T, implying that thermal heating does not considerably influence the field dependence of the measured critical velocities.

What we believe to be the central point of our measurements is the fact that for the two Nb/Py bilayers, the v^* values are much larger than for the Nb single film. Looking at Eq. (4), this must reflect in very different values for the relaxation time τ_E for the two systems. In Fig. 5, the temperature dependence τ_E is given for the single Nb film at two different fields, $\mu_0 H = 0.45$ T above and $\mu_0 H = 0.20$ T below the crossover field to constant v^* at $t = 0.5$. The solid lines are the curves $\tau_E = \tau_{E,el} \exp[m\Delta(T)/k_B T]$ with $\tau_{E,el}$ and m both used as fitting parameters. We obtain $\tau_{E,el} = 9.74 \times 10^{-11}$ s and $m = 1.9$ for $\mu_0 H = 0.45$ T and $\tau_{E,el} = 6.68 \times 10^{-12}$ s and $m = 1.8$ for $\mu_0 H = 0.20$ T. The dashed lines are the fit to the experimental data using the expression $\tau_E \propto T^{-n}$, where for both fields we obtain the unphysical value $n = 9$ for the exponent. The result tells us that electron-electron scattering dominates the energy relaxation in Nb film and that the temperature dependence is due to that of the gap, with $\Delta(0) \approx 1.76 k_B T_c$ as expected from the BCS theory. Moreover, the values for $\tau_{E,el}$ are the right order of magnitude. Similar findings are obtained for the temperature dependence of τ_E in the two Nb/Py bilayers. Figure 5 also shows the temperature dependence of τ_E for the sample NbPy10 at $\mu_0 H = 0.15$ T. The dashed line refers to the power-law fit to experimental data with $n = 5$, again unphysical, and the solid line is the exponential fit. In this case, $\tau_{E,el} = 2.80 \times 10^{-12}$ s, not very different from the number for the Nb film in 0.2 T. The coefficient m , however, turns out to be equal to 1.0, suggesting that the effective gap experienced by the quasiparticles in their relaxation process is only half of the bulk gap. The much larger (critical) velocities for vortices in the bilayer system therefore appear directly related to

the suppression of the superconducting order parameter in the S layer.

V. CONCLUSIONS

We have studied the I - V characteristics at different perpendicular magnetic fields and temperatures for a Nb single film and for two Nb/Py bilayers with different Py thicknesses. Critical currents in Nb/Py samples are much smaller than those measured in the single Nb film. We have also observed sudden jumps in the I - V curves due to an instability of the vortex lattice which could not be ascribed to heating

effects of the samples. The values of the critical velocities connected to the measured instabilities are much larger in Nb/Py with respect to the Nb. The above experimental findings are consistently interpreted as an effect of the strong inhomogeneity of the order parameter in the Nb layer when in contact with the ferromagnet.

ACKNOWLEDGMENT

This work is part of the research program of the “Stichting voor Fundamenteel Onderzoek der Materie (FOM),” which is financially supported by the “Nederlandse Organisatie voor Wetenschappelijk Onderzoek (NWO).”

-
- ¹A. I. Buzdin, *Rev. Mod. Phys.* **77**, 935 (2005).
²E. A. Demler, G. B. Arnold, and M. R. Beasley, *Phys. Rev. B* **55**, 15174 (1997).
³I. A. Garifullin, *J. Magn. Magn. Mater.* **240**, 571 (2002).
⁴V. V. Ryazanov, V. A. Oboznov, A. Yu. Rusanov, A. V. Veretennikov, A. A. Golubov, and J. Aarts, *Phys. Rev. Lett.* **86**, 2427 (2001).
⁵T. Kontos, M. Aprili, J. Lesueur, F. Genet, B. Stephanidis, and R. Boursier, *Phys. Rev. Lett.* **89**, 137007 (2002).
⁶C. Cirillo, A. Rusanov, C. Bell, and J. Aarts, *Phys. Rev. B* **75**, 174510 (2007).
⁷J. M. E. Geers, M. B. S. Hesselberth, J. Aarts, and A. A. Golubov, *Phys. Rev. B* **64**, 094506 (2001).
⁸A. I. Larkin and Yu. N. Ovchinnikov, *Sov. Phys. JETP* **41**, 960 (1976).
⁹W. Klein, R. P. Huebener, S. Gauss, and J. Parisi, *J. Low Temp. Phys.* **61**, 413 (1985).
¹⁰A. V. Samoilov, M. Konczykowski, N.-C. Yeh, S. Berry, and C. C. Tsuei, *Phys. Rev. Lett.* **75**, 4118 (1995).
¹¹C. Villard, C. Peroz, and A. Sulpice, *J. Low Temp. Phys.* **131**, 957 (2003).
¹²C. Peroz and C. Villard, *Phys. Rev. B* **72**, 014515 (2005).
¹³S. G. Doettinger, R. P. Huebener, R. Gerdemann, A. Kühle, S. Anders, T. G. Träuble, and J. C. Villegier, *Phys. Rev. Lett.* **73**, 1691 (1994).
¹⁴S. G. Doettinger, S. Kittelberger, R. P. Huebener, and C. C. Tsuei, *Phys. Rev. B* **56**, 14157 (1997).
¹⁵Z. L. Xiao, P. Voss-de Haan, G. Jakob, and H. Adrian, *Phys. Rev. B* **57**, R736 (1998).
¹⁶Z. L. Xiao, P. Voss-de Haan, G. Jakob, Th. Kluge, P. Haibach, H. Adrian, and E. Y. Andrei, *Phys. Rev. B* **59**, 1481 (1999).
¹⁷B. J. Ruck, J. C. Abele, H. J. Trodahl, S. A. Brown, and P. Lynam, *Phys. Rev. Lett.* **78**, 3378 (1997).
¹⁸B. J. Ruck, H. J. Trodahl, J. C. Abele, and M. J. Geselbracht, *Phys. Rev. B* **62**, 12468 (2000).
¹⁹C. Peroz, C. Villard, A. Sulpice, and P. Butaud, *Physica C* **222-226**, 369 (2002).
²⁰Z. L. Xiao and P. Ziemann, *Phys. Rev. B* **53**, 15265 (1996).
²¹A. I. Bezuglyj and V. A. Shklovskij, *Physica C* **202**, 234 (1992).
²²B. Kalisky, Y. Wolfus, Y. Yeshurun, G. Koren, and R. P. Huebener, *Physica C* **401**, 273 (2004).
²³B. Kalisky, P. Aronov, G. Koren, A. Shaulov, Y. Yeshurun, and R. P. Huebener, *Phys. Rev. Lett.* **97**, 067003 (2006).
²⁴A. Yu. Rusanov, M. Hesselberth, J. Aarts, and A. I. Buzdin, *Phys. Rev. Lett.* **93**, 057002 (2004).
²⁵J. S. Moodera, J. Nowak, and R. J. M. van de Veerdonk, *Phys. Rev. Lett.* **80**, 2941 (1998).
²⁶A. Yu. Rusanov, S. Habraken, and J. Aarts, *Phys. Rev. B* **73**, 060505(R) (2006).
²⁷J. Guimpel, M. E. de la Cruz, F. de la Cruz, H. J. Fink, O. Laborde, and J. C. Villegier, *J. Low Temp. Phys.* **63**, 151 (1986).
²⁸Z. Radovic, L. Dobrosavljevic-Grujic, A. I. Buzdin, and J. R. Clem, *Phys. Rev. B* **38**, 2388 (1988).
²⁹P. Koorevaar, Y. Suzuki, R. Coehoorn, and J. Aarts, *Phys. Rev. B* **49**, 441 (1994).
³⁰N. D. Rizzo, J. Q. Wang, D. E. Prober, L. R. Motowidlo, and B. A. Zeitlin, *Appl. Phys. Lett.* **69**, 2285 (1996).
³¹L. N. Bulaevskii, E. M. Chudnovsky, and M. P. Maley, *Appl. Phys. Lett.* **76**, 2594 (2000).
³²M. Z. Cieplak, X. M. Cheng, C. L. Chien, and H. Sang, *J. Appl. Phys.* **97**, 026105 (2005).
³³J. W. A. Robinson, S. Piano, G. Burnell, C. Bell, and M. G. Blamire, *Phys. Rev. Lett.* **97**, 177003 (2006).